https://doi.org/10.5194/essd-2021-16
Preprint. Discussion started: 29 March 2021

Open Access Earth System Science Data Discussions

Harmonization of global surface ocean pCO2 mapped products and their flux calculations; an improved estimate of the ocean carbon sink

Amanda R. Fay[1], Luke Gregor[2], Peter Landschützer[3], Galen A. McKinley[1], Nicolas Gruber[2], Marion Gehlen[4], Yosuke Iida[5], Goulven G. Laruelle[6], Christian Rödenbeck[7], Jiye Zeng[8]

[1] Columbia University and Lamont Doherty Earth Observatory, Palisades NY, USA
[2] Institute of Biogeochemistry and Pollutant Dynamics, ETH Zurich, Zürich, Switzerland
[3] Max Planck Institute for Meteorology, 20146 Hamburg, Germany
[4] Laboratoire des Sciences du Climat et de l'Environnement, Institut Pierre Simon Laplace, Gif-Sur-Yvette, France
[5] Atmosphere and Ocean Department, Japan Meteorological Agency, 1-3-4 Otemachi, Chiyoda-Ku, Tokyo 100-8122, Japan
[6] Dept. - Geoscience, Environment & Society (DGES), Université Libre de Bruxelles, Bruxelles, CP16002, Belgium
[7] Biogeochemical Signals, Max Planck Institute for Biogeochemistry, P.O. Box 600164, Hans-Knöll-Str. 10, 07745 Jena, Germany
[8] National Institute for Environmental Studies (NIES), 16-2 Onogawa, Tsukuba, Ibaraki, 305-8506, Japan

Correspondence to: Amanda R. Fay (afay@ldeo.columbia.edu)

Abstract. Air-sea flux of carbon dioxide (CO_2) is a critical component of the global carbon cycle and the climate system with the ocean removing about a quarter of the CO_2 emitted into the atmosphere by human activities over the last decade. A common approach to estimate this net flux of CO_2 across the air-sea interface is the use of surface ocean CO_2 observations and the computation of the flux through a bulk parameterization approach. Yet, the details for how this is done in order to arrive at a global ocean CO_2 uptake estimate varies greatly, unnecessarily enhancing the uncertainties. Here we reduce some of these uncertainties by harmonizing an ensemble of products that interpolate surface ocean CO_2 observations to near global coverage. We propose a common methodology to fill in missing areas in the products and to calculate fluxes and present a new estimate of the net flux. The ensemble data product, SeaFlux (Gregor & Fay (2021), doi.org/10.5281/zenodo.4133802, https://github.com/luke-gregor/SeaFlux), accounts for the diversity of the underlying mapping methodologies. Utilizing six global observation-based mapping products (CMEMS-FFNN, CSIR-ML6, JENA-MLS, JMA-MLR, MPI-SOMFFN, NIES-FNN), the SeaFlux ensemble approach adjusts for methodological inconsistencies in flux calculations that can result in an average error of 15% in global mean flux estimates. We address differences in spatial coverage of the surface ocean CO_2 between the mapping products which ultimately yields an increase in CO_2 uptake of up to 19% for some products. Fluxes are calculated using three wind products (CCMPv2, ERA5, and JRA55). Application of an appropriately scaled gas exchange coefficient has a greater impact on the resulting flux than solely the choice of wind product. With these adjustments, we derive an improved ensemble of surface ocean pCO_2 and air-sea carbon flux estimates. The SeaFlux ensemble suggests a

https://doi.org/10.5194/essd-2021-16
Preprint. Discussion started: 29 March 2021

global mean uptake of CO_2 from the atmosphere of 1.92 +/- 0.35 PgC yr^{-1}. This work aims to support the community effort to perform model-data intercomparisons which will help to identify missing fluxes as we strive to close the global carbon budget.

1 Introduction

Surface ocean partial pressure of CO_2 (pCO_2) observations play a key role in constraining the global ocean carbon sink. This is because variations in surface ocean pCO_2 is the driving force governing the exchange of CO_2 across the air-sea interface, which is commonly described through a bulk formula (Garbe et al. 2014; Wanninkhof 2014):

$$\text{Flux} = k_w \cdot sol \cdot (p\text{CO}_2 - p\text{CO}_2^{\text{atm}}) \cdot (1 - ice) \qquad (1)$$

where k_w is the gas transfer velocity, *sol* is the solubility of CO_2 in seawater, in units mol m^{-3} μatm^{-1}, $p\text{CO}_2$ is the partial pressure of surface ocean CO_2 in µatm, and $p\text{CO}_2^{\text{atm}}$ in units of µatm represents the partial pressure of atmospheric CO_2 in the marine boundary layer. Finally, to account for the seasonal ice cover in high latitudes the fluxes are weighted by 1 minus the ice fraction (*ice*), *i.e.* the open ocean fraction.

With the increasing number of observations of pCO_2 available in each new release of the Surface Ocean Carbon Dioxide Atlas (SOCAT; Bakker et al. 2016) and the adoption of various pCO_2 mapping techniques, multiple observation-based estimates of the pCO_2 field are now publicly available and updated on an annual basis. Despite these advancements, the intercomparison of the products' flux values is hindered (1) by different areal coverage and (2) by a lack of a systematic approach to calculate the sea-air CO_2 flux from pCO_2 (Table A1). These differences in flux calculations introduce uncertainty in comparisons between the products as well as with their comparisons to Global Ocean Biogeochemistry Models (GOBM). In this work, we harmonize these product's flux estimates, specifically addressing three key differences between product methodologies. The resulting flux estimates can then be more meaningfully compared.

The first step addresses the variable spatial coverage of current pCO_2 products. Some of the current mapped products only cover roughly 90% of the ocean surface, missing coastal and high latitude regions. A newly released global pCO_2 climatology product (Landschützer et al. 2020b) includes coverage in the coastal and Arctic regions. We use this climatology to fill any missing areas in each individual product to create a consistent full global ocean coverage.

The second methodological step is the choice of flux parameterization, and appropriate scaling of wind speed data. Roobaert et al. (2018) present uncertainty in air-sea carbon flux induced by various parameterizations of the gas transfer velocity and

https://doi.org/10.5194/essd-2021-16
Preprint. Discussion started: 29 March 2021

wind speed data products. Utilizing the MPI-SOMFFN pCO_2 product (Landschützer et al. 2020a) and a quadratic parameterization (Wanninkhof 1992) they find flux estimates that diverge by 12% depending on the choice of wind speed products. Additionally, they find regional discrepancies to be much more pronounced than global differences, specifically highlighting the equatorial Pacific, Southern Ocean, and North Atlantic as regions most impacted by the choice of wind product. Roobaert et al. (2018) stress that to minimize the uncertainties associated with the wind speed product chosen, the global coefficient of gas transfer must be individually calculated for each (Wanninkhof 1992, 2014). In this work, we assess the impact of wind speed product choice and scaling on six pCO_2 products' calculated air-sea flux estimates. By applying a consistent flux calculation methodology to each pCO_2 product, we minimize the methodological divergence of fluxes within the ensemble.

SeaFlux provides a more consistent approach specifically targeting the most commonly used pCO_2 data products to deliver an end product for consistent intercomparisons within assessment studies such as the Global Carbon Budget (Friedlingstein et al. 2020; Hauck et al. 2020). By first addressing differences in spatial coverage between the observation-based products we are able to better present a true global pCO_2 estimate for each product. This SeaFlux package also provides a means to normalize the gas transfer velocity to a consistent ^{14}C inventory. By calculating fluxes using multiple scaled gas transfer velocities for different wind products, we present a methodologically consistent database of air-sea CO_2 fluxes. The SeaFlux package is an ensemble data product along with documented code allowing the community to reproduce consistent flux calculations from various data-based pCO_2 reconstructions.

2. Methods

The SeaFlux method is based on six observation-based pCO_2 products and spans years 1988-2018 (Table 1). These six include three neural network derived products (MPI-SOMFFN, CMEMS-FFNN, NIES-FNN), a mixed layer scheme product (JENA-MLS), a multiple linear regression (JMA-MLR), and a machine learning ensemble (CSIR-ML6). These select products are included as they have been regularly updated to extend their time period and incorporate additional data that comes with each annual release of the SOCAT database.

All of these methods provide full three-dimensional fields (latitude, longitude, time) of the sea surface partial pressure of CO_2 (pCO_2) and the air-sea CO_2 flux. In their original form each product may utilize different choices for the inputs to Equation 1 (Table A1). In this work recompute the fluxes using the following inputs to the bulk parameterization approach Equation 1: k_w is the gas transfer velocity (further discussed in Sect. 2.3), *sol* is the solubility of CO_2 in seawater, in units mol m^{-3} $uatm^{-1}$, calculated using the formulation by Weiss (1974), EN4 salinity (Good et al. 2013), Operational Sea Surface Temperature and Sea Ice Analysis (OSTIA) sea surface temperature (Good et al. 2020), and European Centre for Medium-Range Weather Forecasts (ECMWF) ERA5 sea level pressure (Hersbach et al. 2020); *ice* is the sea ice fraction from OSTIA

https://doi.org/10.5194/essd-2021-16
Preprint. Discussion started: 29 March 2021

(Good et al. 2020); pCO_2 is the partial pressure of oceanic CO_2 in μatm for each observation-based product after filling as discussed in Sect. 2.1, and pCO_2^{atm} is the dry air mixing ratio of atmospheric CO_2 (xCO_2) from the ESRL surface marine boundary layer CO_2 product available at https://www.esrl.noaa.gov/gmd/ccgg/mbl/data.php (Dlugokencky et al. 2017) multiplied by ERA5 sea level pressure (Hersbach et al. 2020) at monthly resolution, and applying the water vapor correction according to Dickson et al. (2007).

Flux is defined positive upward, i.e., CO_2 release from the ocean into the atmosphere is positive, and uptake by the ocean is negative. In the following sections we discuss the three steps that have the greatest impact on the inconsistencies between unadjusted flux calculations in the six pCO_2 products and the approach that we utilize for the SeaFlux ensemble product.

2.1 Step 1: Area filling

Machine learning methods aim to maximize the utility of the existing in situ observations by extrapolation using various proxy variables for processes influencing changes in ocean pCO_2. Extrapolation with these independently observed variables is possible due to the nonlinear relationship between pCO_2 in the surface ocean and the proxies that drive these changes. However, not all of the proxy variables have complete global ocean coverage for all months, so the resulting pCO_2 products are limited by the extent of the proxy variables (Figure 1). Additionally, in coastal regions there is the potential that different relationships of pCO_2 are expected than in the open ocean, thus limiting the extrapolations. In contrast, the mixed layer scheme (utilized by the JENA-MLS product) does not suffer from such missing areas but does not distinguish between coastal and open ocean. While the area extent of the available air-sea flux estimates varies between products, there are consistent patterns; nearly all products cover the open ocean, whereas larger differences exist in the coverage of coastal regions, shelf seas, marginal seas and the Arctic Ocean.

To account for differing area coverage, past studies (Friedlingstein et al. 2019, 2020; Hauck et al. 2020) have adjusted simply by scaling based on the percent of the total ocean area covered by each observation-based product. This does not account for the fact that some areas have CO_2 flux densities that are higher or lower than the global average (Table 1,3). Thus, the magnitude of the adjustment by area-scaling is likely an underestimate (McKinley et al. 2020). One specific example is the northern high latitudes where coverage by the six products varies substantially. Similarly, three products provide estimates in marginal seas such as the Mediterranean while the other three products have no reported pCO_2 values here. Shutler et al (2016) report that subtle differences in regional definitions can cause differences of >10% in the calculated net fluxes.

To address the inconsistent spatial coverage in products we utilize a newly released open and coastal merged climatology product (MPI-ULB-SOMFFN; Landschützer et al. 2020b) that is a blend of the coastal ocean SOMFFN mapping method (Laruelle et al. 2017) and the open ocean equivalent (MPI-SOMFFN; Landschützer et al. 2020a), but which now includes

https://doi.org/10.5194/essd-2021-16
Preprint. Discussion started: 29 March 2021

missing coastal ocean regions, marginal seas and the full Arctic Ocean. For each observationally-based product, we fill missing grid cells with a scaled value based on this global-coverage climatology (Figure 2). The scaling accounts for year-to-year changes in pCO_2 in the missing areas (given that the extended MPI-ULB-SOMFFN product is a monthly climatology centered on year 2006) and is obtained as follows.

To extend the open and coastal merged monthly climatology (MPI-ULB-SOMFFN) to 1988-2018, we calculate a global scaling factor based on the product-based ensemble mean pCO_2 for regions which are covered consistently by all six pCO_2 products. We first mask all pCO_2 products to a common sea mask before taking an ensemble mean (pCO_2^{ens}). Next, we divide this ensemble mean by the MPI-ULB-SOMFFN climatology (pCO_2^{clim}) at monthly 1° by 1° resolution (Equation 2). The monthly scaling factor (sf_{pCO2}) is calculated by taking the mean over the spatial dimensions.

The scaling factor calculation can be represented as

$$sf_{pCO_2} = mean_{x,y}\left(\frac{pCO_2^{ens}}{pCO_2^{clim}}\right) \qquad (2)$$

where sf_{pCO_2} is the one-dimensional scaling factor (time dimension), pCO_2^{ens} is the ensemble mean of all pCO_2 products at three-dimension, monthly 1° by 1° resolution, pCO_2^{clim} is the MPI-ULB-SOMFFN climatology, also at three-dimension but limited to just one climatological year. The *x* and *y* indicate that we take the area-weighted average over longitude (*x*) and latitude (*y*) resulting in the monthly scaling value. If a product mean is exactly equal to the climatology mean, the scaling factor is 1. Value ranges from 0.91 to 1.06 over the 31-year time period.

The one-dimensional scaling factor is then multiplied by the MPI-ULB-SOMFFN climatology for each spatial point resulting in a three-dimensional scaled filling map. These values are then used to fill in missing grid cells in each observation-based product.

Globally, the adjustments are all less than 20% of the total flux, with the mean adjustment for the six products at 9%. In the Northern Hemisphere however, the filling process can drive adjustments of up to 35% (Table 3). As expected, the observationally-based products with more complete spatial coverage tend to have smaller flux adjustments, however the impact on the final CO_2 flux depends on the ΔpCO_2 and wind speed of the areas being filled (Figures 2-3, Table 1,3). The only product that does not change during this adjustment process is the JENA-MLS mixed layer scheme-based product (Rödenbeck et al. 2013) which is produced with full spatial coverage and therefore needs no spatial filling.

Our approach is not without its own assumptions and limitations. We rely on a single estimate of the missing pCO_2 in coastal ocean regions, marginal seas, and the full Arctic Ocean, given that this is the only publicly available product currently

https://doi.org/10.5194/essd-2021-16
Preprint. Discussion started: 29 March 2021

existing. Nevertheless, the fact that common missing areas along coastal regions and marginal seas are reconstructed using specific coastal observations provides a step forward from the linear-scaling approach currently used by the Global Carbon Budget (Friedlingstein et al. 2019, 2020). Further confidence is provided by previous research showing that climatological relevant signals, i.e. mean state and seasonality, are well reconstructed by the MPI-SOMFFN method (Gloege et al. 2021).

Furthermore, our scaled filling methodology assumes that pCO_2 in the missing ocean regions is increasing at the same rate as the common area of open-ocean pCO_2 used to calculate the scaling factor. Research from coastal ocean regions and shelf seas reveal that, in spite of a large spatial heterogeneity, this is a reasonable first order approximation (Laruelle et al. 2018). While our approach has a constant scaling factor for the missing ocean areas regardless of latitude we acknowledge that this could be improved with increased understanding.

2.2 Step 2: Wind product selection

Historical wind speed observations (including measurements from satellites and moored buoys) are aggregated and extrapolated through modeling and data assimilation systems to create global wind reanalyses. These reanalyses are required to compute =air-sea gas exchange. Air-sea flux is commonly parameterized as a function of the gradient of CO_2 between the ocean and the atmosphere with wind speed modulating the rate of the gas exchange (Equation 1). Each of these wind reanalyses has strengths and weaknesses, specifically on regional and seasonal scales (Chaudhuri et al. 2014; Ramon et al. 2019) but all are considered reasonable options by the community (Roobaert et al. 2018). We use three wind reanalysis products for completeness: the Cross-Calibrated Multi-Platform v2 (CCMP2, Atlas et al. 2011), the Japanese 55-year Reanalysis (JRA-55, Kobayashi et al. 2015), and the European Centre for Medium-Range Weather Forecasts (ECMWF) ERA5 (Hersbach et al. 2020). The wind speed (U_{10}) is calculated at the native resolution of each wind product from the u- and v-components of wind. Details of each wind product are shown in Table A2.

2.3 Step 3: Calculation of gas exchange coefficient

We employ the quadratic windspeed dependence of the gas transfer velocity (Wanninkhof 1992) and calculate the piston velocity (*kw*) for each of the wind reanalysis products as

$$k_w = a \cdot \langle U^2 \rangle \cdot \left({}^{Sc}/_{660}\right)^{-0.5} \tag{3}$$

where the units of k_w are in cm h^{-1}, *Sc* is the dimensionless Schmidt number, and $\langle U^2 \rangle$ denotes the second moment of average 10-m height winds (m s^{-1}). We choose the quadratic dependence of the gas transfer velocity as it is widely accepted and used in the literature (Wanninkhof, 1992). Observational and modeling studies have often suggested that different

https://doi.org/10.5194/essd-2021-16
Preprint. Discussion started: 29 March 2021

parametrizations could be more appropriate under specific conditions (Fairall et al. 2000; Nightingale et al. 2000; McGillis et al. 2001; Krakauer et al. 2006); however, recent direct carbon dioxide flux measurements made in the high latitude Southern Ocean confirm that even in this high wind environment, a quadratic parameterization fits the observations best (Butterworth & Miller 2016). Future updates of the SeaFlux product will include options for other parameterizations.

We calculate the square of the wind speed at the native resolution of each wind product and then average it to 1° by 1° monthly resolution (see Table A2). The order of this calculation is important as information is lost when resampling data to lower resolutions because of the concavity of the quadratic function. For example, if the second moment were calculated from time-averaged wind speeds, it would result in an underestimate of the gas transfer velocity (Sarmiento and Gruber 2006; Sweeney et al. 2007). The resulting second moment is equivalent to $\langle U^2 \rangle = U_{mean}^2 + U_{std}^2$ where U_{mean} and U_{std} are the temporal mean and standard deviation calculated from the native temporal resolution of U.

In addition to the choice of wind parameterization, large differences in flux can result due to the scaling coefficient of gas transfer (*a*) that is applied when calculating the global mean piston velocity. This constant originates from the gas exchange process studies (Krakauer et al. 2006; Sweeney et al. 2007; Müller et al. 2008; Naegler 2009) which utilize observations of radiocarbon data from the GEOSECS and WOCE/JGOFS expeditions (Key et al. 2004). The ^{14}C released from nuclear bomb testing (hence bomb-^{14}C) in the mid twentieth century has since been taken up by the ocean. The number of bomb-^{14}C atoms in the ocean, relative to the pre-bomb ^{14}C, can thus be used as a constraint on the long-term rate of exchange of carbon between the atmosphere and the ocean. A probability distribution of wind speed is used to optimize the coefficient of gas transfer based on these observed natural and bomb ^{14}C invasion rates. This coefficient must be individually calculated and is not consistent for each wind product. Further, the gas transfer velocity used by the different pCO_2 mapping products are not scaled to the same bomb-^{14}C estimate (Table A1). The range of the different bomb-^{14}C estimates is within the range of the uncertainty from the associated studies (Naegler, 2009), but the choice would introduce inconsistency that is easily addressed here.

We scale the gas transfer velocity to a bomb-^{14}C flux estimate of 16.5 cm hr^{-1} as recommended by Naegler (2009). The coefficient (*a*) is calculated for each wind product via a cost function which optimizes the coefficient of gas transfer

$$a = k_w \cdot \langle U^2 \rangle^{-1} \cdot \left({Sc}/{660} \right)^{0.5} \cdot (1 - ice) \tag{4}$$

where parameters are as defined in Equation 3. The units of the coefficient *a* are (cm h^{-1}) (m s^{-1})$^{-2}$. Global winds from the wind speed products differ and therefore even with the same bomb-^{14}C observations the scaled coefficient (*a*) can have a

https://doi.org/10.5194/essd-2021-16
Preprint. Discussion started: 29 March 2021

40% range (Wanninkhof 2014). By determining the optimal *a* coefficient for each of the reanalysis winds, uncertainty in the global fluxes can be decreased. Our scaled coefficients (Table 2) correspond well with the estimate of Wanninkhof (2014) who uses the CCMP wind product to estimate *a* as 0.251. Differences in the coefficient will also result from the time period considered and definition of global area and ice fraction applied in the calculation.

This scaling of the gas exchange coefficient (*a*) for each wind product is an essential, and an inconsistently applied step (Table A1), that has large implications for air-sea flux estimates (Figure 4). Without individual scaling, and instead utilizing a set value for the gas transfer coefficient (*a*) regardless of wind product, our results show that calculated global fluxes could be as high as 9% different depending on which pCO_2 and wind reanalysis product considered (Roobaert et al. 2018).

2.4 Further parameters for flux calculation

The remaining parameters of Equation 1 are the solubility of CO_2 in seawater (*sol*), the atmospheric partial pressure of CO_2 (pCO_2^{atm}), and the area weighting to account for sea ice cover. While the choices of products used for these parameters can also result in differences in flux estimates, the impacts are much smaller as compared with the parameters discussed above.

Atmospheric pCO_2 is calculated as the product of surface xCO_2 and sea level pressure corrected for the contribution of water vapor pressure. The choice of the sea level pressure product, or absence of the water vapor correction can have small, but not insignificant, impact on the calculated fluxes. Additionally, some products utilize the output of an atmospheric CO_2 inversion product (*e.g.* CarboScope, Rödenbeck et al. 2013; CAMS CO_2 inversion, Chevallier, 2013) which can introduce differences in the flux estimate outside of the sources related to a product's surface ocean pCO_2 mapping method. Importantly, we do not advocate that our estimate of pCO_2^{atm} is an improvement over other estimates thereof; rather we provide an estimate of pCO_2^{atm} that has few assumptions and leads to a methodologically consistent estimate of ΔpCO_2. We maintain the same philosophy in our estimates of solubility of CO_2 in seawater and sea-ice area weighting and therefore we do not elaborate on them here.

3. Results and Discussion

3.1 SeaFlux air-sea CO_2 flux calculation

Following Equation 1, CO_2 flux is calculated individually for each of the six observation-based products with each available wind product (CCMPv2, ERA5, JRA55) as discussed in Sect. 2.2 (Table 4). Since we account for spatial coverage differences via our filling method (Sect. 2.1), taking a global mean flux for each of the data products is now straight forward. Figure 4 shows the difference these wind products generate on the resulting global mean flux of the CSIR-ML6 product as

https://doi.org/10.5194/essd-2021-16
Preprint. Discussion started: 29 March 2021

one example (other products in Figure A2). The three wind products show very consistent fluxes throughout the time series, however the importance of appropriate scaling of the gas exchange coefficient (*a*) is evident by the significant differences between global mean fluxes calculated with unscaled and scaled *a* value (Figure 4). It is clear that the impact of applying the appropriate gas exchange coefficient through proper scaling has a larger impact on the resulting flux time series than solely the choice of wind product.

3.2 SeaFlux ensemble flux

By calculating each product's flux using these consistent methods, we permit for a more accurate comparison of fluxes and increase confidence in the SeaFlux product ensemble mean flux estimate of -1.92 +/- 0.35 PgC yr^{-1} (Table 4). Here, the stated uncertainty represents 2σ as calculated from the 18 realizations of flux included in the SeaFlux ensemble (six pCO_2 products and three wind products). This result is further strengthened by the use of multiple wind products which we consider to be independent estimates for the purpose of the uncertainty calculation.

These flux values will be different from those produced by the observation-based pCO_2 product's original creator, both spatially and on the mean (Figure 5, Table A1, A3). However, by calculating fluxes using this standardized approach we have higher confidence in the uncertainties and in the ensemble mean of global fluxes.

3.3 Issues not addressed by SeaFlux

While the SeaFlux data set allows us to standardize much of the calculation of air-sea carbon flux, the community is still working towards consensus on other issues that impact this estimate. One source of uncertainty has been raised by Watson et al. (2020) who contend that a correction should be applied to pCO_2 observations to account for the vertical temperature gradient between the ship water intake depth and the surface skin layer where gas exchange actually takes place. A further correction should be applied when calculating fluxes to account for the "cool skin" effect caused by evaporation (Woolf et al. 2016; Watson et al. 2020). Applying these corrections results in an increasing CO_2 sink by up to 0.9 PgC yr^{-1} (Watson et al. 2020). Here, we do not take such corrections into account for two reasons. Firstly, the skin temperature correction to pCO_2 needs to be applied directly to the measurements and not the final interpolated pCO_2 from the data products. Hence, it is up to the developers of the SOCAT dataset and the developers of the pCO_2 mapping products to decide on the inclusion of this correction. It would then be up to the developers of the data products to update their mapped products. Secondly, the cool skin correction would be equally applied to all methods and would not contribute to the inconsistencies that we are trying to address here. As the ocean carbon community moves towards consensus on such issues, the SeaFlux product will be updated to include revised protocols.

To compare these estimates of contemporary air-sea net flux (Fnet) from surface ocean pCO_2 with estimates of the anthropogenic carbon flux (Fant) from interior data (Mikaloff Fletcher et al. 2006; DeVries 2014; Gruber et al. 2019), or from global ocean biogeochemical models (Friedlingstein et al. 2020; Hauck et al. 2020), it is necessary to account for the

https://doi.org/10.5194/essd-2021-16
Preprint. Discussion started: 29 March 2021

outgassing of natural carbon which was supplied to the ocean by rivers as well as the non-steady state behavior of the natural carbon cycle (Hauck et al. 2020). Work is ongoing to quantify the lateral river carbon flux transported into the coastal and open oceans. Current estimates are 0.23 PgC yr^{-1} (Lacroix et al. 2020),0.45 PgC yr^{-1} (Jacobsen et al. 2007), and 0.78 PgC yr^{-1} (Resplandy et al. 2018) with the regional distribution of these inputs remaining unclear (Aumont et al. 2001; Lacroix et al. 2020). Quantification of non-steady state behavior of the natural carbon cycle has only recently been proposed and significant uncertainty remains, with a magnitude range of 0.05-0.4 PgC/yr for 1994-2007 (Gruber et al. 2019, McKinley et al. 2020). Similar to the "cool skin" correction suggested by Watson et al. (2020) discussed above, in this work we have not included a revision for this riverine input as it would not contribute to the inconsistencies between the different products for Fnet itself, which is our focus.

4. Data Availability

Data (Gregor & Fay 2021) is available on Zenodo (https://doi.org/10.5281/zenodo.4133802) and the software used to generate this data is available on GitHub (https://github.com/luke-gregor/SeaFlux).

5. Conclusions

We introduce a standardized approach for flux calculations from observationally-based pCO_2 products. The SeaFlux approach for flux calculations from available surface ocean pCO_2 estimates enhances consistency and comparability for this ensemble of products. Specifically, we address the two largest sources of divergence, namely the differences in spatial coverage between the products, and the scaling of the gas transfer velocity for available wind speed products based on global ^{14}C-based constraints. The area adjustment is the largest contributor to the methodological discrepancies, resulting in an increase in CO_2 uptake of 0-20% relative to the original, possibly incomplete coverage (depending on pCO_2 product). The global scaling of the gas transfer velocity can change the CO_2 flux on average by 6% relative to non-standardized flux calculations. The impact of applying the appropriate gas exchange coefficient through proper scaling has a larger impact on the resulting flux time series than solely the choice of wind product. By accounting for these sources of differences, the global mean calculated air-sea carbon flux calculated from the six available products is adjusted by up to 24%. The ensemble mean air-sea carbon flux is estimated to be -1.92 +/- 0.35 PgC yr^{-1} with the uncertainty representing 2σ as calculated from the 18 realizations.

This work provides an ensemble data product of the sea-air CO_2 flux based on observation-based pCO_2 products. This ensemble product is meant to facilitate the use of the pCO_2 observation-based ocean flux estimates in assessment studies of the global carbon cycle, such as the Global Carbon Budget or RECCAP-2. In addition to enhanced consistency, our area correction and the consistent scaling of gas exchange may help reduce the current carbon budget imbalance (Friedlingstein et al. 2019, 2020). Note that the original sea-air CO_2 flux products still offer additional information important in other

https://doi.org/10.5194/essd-2021-16
Preprint. Discussion started: 29 March 2021

applications, such as coverage over longer time periods, higher spatial or temporal resolution, or runs incorporating further auxiliary data sets or pCO_2 data (e.g., SOCCOM float data, Bushinsky et al. 2019).

Along with the ensemble of CO_2 flux fields, we also provide a public-use coding package allowing users to apply the presented standardized flux calculations to own data-based pCO_2 reconstructions.

Author Contributions

ARF and LG designed the experiment and LG developed the model code and performed the simulations with ARF focusing on analysis. ARF prepared the manuscript with contributions from all co-authors.

Acknowledgements

P.L, N.G and L.G received funding from the European Community's Horizon 2020 Project under grant agreement no. 821003 (4C). The Surface Ocean CO_2 Atlas (SOCAT) is an international effort, endorsed by the International Ocean Carbon Coordination Project (IOCCP), the Surface Ocean Lower Atmosphere Study (SOLAS) and the Integrated Marine Biosphere Research (IMBeR) program, to deliver a uniformly quality-controlled surface ocean CO_2 database. The many researchers and funding agencies responsible for the collection of data and quality control are thanked for their contributions to SOCAT.

References

Atlas, R., Hoffman, R.N., Ardizzone, J., Leidner, S.M., Jusem, J.C., Smith, D.K. and Gombos, D.: A cross-calibrated, multiplatform ocean surface wind velocity product for meteorological and oceanographic applications. *Bulletin of the American Meteorological Society*, *92*(2), pp.157-174, https://doi.org/10.1175/2010BAMS2946.1, 2011.

Aumont, O., Orr, J. C., Monfray, P., Ludwig, W., Amiotte-Suchet, P., and Probst, J.-L.: Riverine-driven interhemispheric transport of carbon, *Global Biogeochem. Cycles*, 15(2), 393– 405, doi:10.1029/1999GB001238, 2001.

Bakker, D. C. E., Pfeil, B., Landa, C. S., Metzl, N., O'Brien, K.M., Olsen, A., Smith, K., Cosca, C., Harasawa, S., Jones, S. D., Nakaoka, S., Nojiri, Y., Schuster, U., Steinhoff, T., Sweeney, C., Takahashi, T., Tilbrook, B., Wada, C., Wanninkhof, R., Alin, S. R., Balestrini, C. F., Barbero, L., Bates, N. R., Bianchi, A. A., Bonou, F., Boutin, J., Bozec, Y., Burger, E. F., Cai, W.-J., Castle,
R. D., Chen, L., Chierici, M., Currie, K., Evans, W., Featherstone, C., Feely, R. A., Fransson, A., Goyet, C., Greenwood, N., Gregor, L., Hankin, S., Hardman-Mountford, N. J., Harlay, J., Hauck, J., Hoppema, M., Humphreys, M. P., Hunt, C. W.,

Huss, B., Ibánhez, J. S. P., Johannessen, T., Keeling, R., Kitidis, V., Körtzinger, A., Kozyr, A., Krasakopoulou, E., Kuwata, A., Landschützer, P., Lauvset, S. K., Lefèvre, N., Lo Monaco, C., Manke, A., Mathis, J. T., Merlivat, L., Millero, F. J., Monteiro, P. M. S., Munro, D. R., Murata, A., Newberger, T., Omar, A. M., Ono, T., Paterson, K., Pearce, D., Pierrot, D., Robbins, L. L., Saito, S., Salisbury, J., Schlitzer, R., Schneider, B., Schweitzer, R., Sieger, R., Skjelvan, I., Sullivan, K. F., Sutherland, S. C., Sutton, A. J., Tadokoro, K., Telszewski, M., Tuma, M., van Heuven, S. M. A. C., Vandemark, D.,Ward, B.,Watson, A. J., and Xu, S.: A multidecade record of high-quality fCO2 data in version 3 of the Surface Ocean CO2 Atlas (SOCAT), Earth Syst. Sci. Data, 8, 383–413, https://doi.org/10.5194/essd-8-383-2016, 2016.

Bakker, D. C. E., Alin, S. R., Bates, N., Becker, M., Castaño-Primo, R., Cosca, C. E., Cronin, M., Kadono, K., Kozyr, A., Lauvset, S. K., Metzl, N., Munro, D. R., Nakaoka, S., O'Brien, K. M., Ólafsson, J., Olsen, A., Pfeil, B., Pierrot, D., Smith, K., Sutton, A. J., Takahashi, T., Tilbrook, B., Wanninkhof, R., Andersson, A., Atamanchuk, D., Benoit-Cattin, A., Bott, R., Burger, E. F., Cai, W.-J., Cantoni, C., Collins, A., Corredor, J. E., Cronin, M. F., Cross, J. N, Currie, K. I., De Carlo, E. H., DeGrandpre, M. D., Dietrich, C., Emerson, S., Enright, M. P., Evans, W., Feely, R. A., García-Ibáñez, M. I., Gkritzalis, T., Glockzin, M., Hales, B., Hartman, S. E., Hashida, G., Herndon, J., Howden, S. D., Humphreys, M. P., Hunt, C. W., Jones, S. D., Kim, S., Kitidis, V., Landa, C. S, Landschützer, P., Lebon, G. T., Lefèvre, N., Lo Monaco, C., Luchetta, A., Maenner Jones, S., Manke, A. B., Manzello, D., Mears, P., Mickett, J., Monacci, N. M., Morell, J. M., Musielewicz, S., Newberger, T., Newton, J., Noakes, S.,
Noh, J.-H., Nojiri, Y., Ohman, M., Ólafsdóttir, S., Omar, A. M., Ono, T., Osborne, J., Plueddemann, A. J., Rehder, G., Sabine, C.
L, Salisbury, J. E., Schlitzer, R., Send, U., Skjelvan, I., Sparnocchia, S., Steinhoff, T., Sullivan, K. F., Sutherland, S. C., Sweeney, C., Tadokoro, K., Tanhua, T., Telszewski, M., Tomlinson, M., Tribollet, A., Trull, T., Vandemark, D., Wada, C., Wallace, D. W. R., Weller, R. A., and Woosley, R. J.: Surface Ocean CO2 Atlas Database Version 2020 (SOCATv2020) (NCEI Accession 0210711), NOAA National Centers for Environmental Information, https://doi.org/10.25921/4xkx-ss49. 2020.

Bushinsky, S.M., Landschützer, P., Rödenbeck, C., Gray, A.R., Baker, D., Mazloff, M.R., Resplandy, L., Johnson, K.S. and Sarmiento, J.L.: Reassessing Southern Ocean air-sea CO2 flux estimates with the addition of biogeochemical float observations. *Global biogeochemical cycles*, *33*(11), pp.1370-1388, https://doi.org/10.1029/2019GB006176, 2019.

Butterworth, B. J., Miller, S. D.: Air-sea exchange of carbon dioxide in the Southern Ocean and Antarctic marginal ice zone, Geophys. Res. Lett., 43, 7223–7230, doi:10.1002/2016GL069581, 2016.

Chau, T. T., Gehlen, M., and Chevallier, F.: Global Ocean Surface Carbon Product MULTIOBS_ GLO_BIO_CARBON_SURFACE_REP_015_008, E.U. Copernicus Marine Service Information, available at:

https://doi.org/10.5194/essd-2021-16
Preprint. Discussion started: 29 March 2021

https://resources.marine.copernicus.eu/documents/PUM/CMEMS-MOB-PUM-015-008.pdf, last access: 11 January 2021.

Chaudhuri, A.H., Ponte, R.M. and Nguyen, A.T.: A comparison of atmospheric reanalysis products for the Arctic Ocean and implications for uncertainties in air–sea fluxes. *Journal of climate*, *27*(14), pp.5411-5421, https://doi.org/10.1175/JCLI-D-13-00424.1, 2014.

Chevallier, F.: On the parallelization of atmospheric inversions of CO2 surface fluxes within a variational framework, Geosci. Model Dev., 6, 783–790, https://doi.org/10.5194/gmd-6-783-2013, 2013

Copernicus Climate Change Service (C3S): ERA5: Fifth generation of ECMWF atmospheric reanalyses of the global climate . Copernicus Climate Change Service Climate Data Store (CDS), *date of access*. https://cds.climate.copernicus.eu/cdsapp#!/home. 2017.

Denvil-Sommer, A., Gehlen, M., Vrac, M., and Mejia, C.: LSCEFFNN-v1: a two-step neural network model for the reconstruction of surface ocean pCO2 over the global ocean, Geosci. Model Dev., 12, 2091–2105, https://doi.org/10.5194/gmd-12-2091-2019, 2019.

DeVries, T.: The oceanic anthropogenic CO_2 sink: Storage, air-sea fluxes, and transports over the industrial era, *Global Biogeochem. Cycles*, 28, 631– 647, doi:10.1002/2013GB004739, 2014)

Dickson, A. G., Sabine, C. L., and Christian, J. R. (Eds.): Guide to best practices for ocean CO2 measurements, PICES Special Publication 3, IOCCP Report 8, 191 pp., 2007.

Dlugokencky, E. and Tans, P.: Trends in atmospheric carbon dioxide, National Oceanic and Atmospheric Administration, Earth System Research Laboratory (NOAA/ESRL), available at: http://www.esrl.noaa.gov/gmd/ccgg/trends/global.html, last access: 16 October 2020.

Fairall, C.W., Hare, J. E., Edson, J. B. and McGillis,W.: Parameterization and micrometeorological measurement of air-sea gas transfer. Boundary-Layer Meteorology 96(1–2), 63–105, https://doi.org/10.1023/A:1002662826020, 2000.

Friedlingstein, P., Jones, M. W., O'Sullivan, M., Andrew, R. M., Hauck, J., Peters, G. P., Peters, W., Pongratz, J., Sitch, S., Le Quéré, C., Bakker, D. C. E., Canadell, J. G., Ciais, P., Jackson, R. B., Anthoni, P., Barbero, L., Bastos, A., Bastrikov, V., Becker, M., Bopp, L., Buitenhuis, E., Chandra, N., Chevallier, F., Chini, L. P., Currie, K. I., Feely, R. A., Gehlen, M., Gilfillan, D., Gkritzalis, T., Goll, D. S., Gruber, N., Gutekunst, S., Harris, I., Haverd, V., Houghton, R. A., Hurtt, G., Ilyina, T., Jain, A. K., Joetzjer, E., Kaplan, J. O., Kato, E., Klein Goldewijk, K., Korsbakken, J. I., Landschützer, P., Lauvset, S. K., Lefèvre, N., Lenton, A., Lienert, S., Lombardozzi, D., Marland, G., McGuire, P. C., Melton, J. R., Metzl, N., Munro, D. R., Nabel, J. E. M. S., Nakaoka, S.-I., Neill, C., Omar, A. M., Ono, T., Peregon, A., Pierrot, D., Poulter, B., Rehder, G., Resplandy, L., Robertson, E., Rödenbeck, C., Séférian, R., Schwinger, J., Smith, N., Tans, P. P., Tian, H., Tilbrook, B., Tubiello, F. N., van der Werf, G. R., Wiltshire, A. J., and Zaehle, S.: Global Carbon Budget 2019, Earth Syst. Sci. Data, 11, 1783–1838, https://doi.org/10.5194/essd-11-1783-2019, 2019.

Friedlingstein, P., O'Sullivan, M., Jones, M. W., Andrew, R. M., Hauck, J., Olsen, A., Peters, G. P., Peters, W., Pongratz, J., Sitch, S., Le Quéré, C., Canadell, J. G., Ciais, P., Jackson, R. B., Alin, S., Aragão, L. E. O. C., Arneth, A., Arora, V., Bates, N. R., Becker, M., Benoit-Cattin, A., Bittig, H. C., Bopp, L., Bultan, S., Chandra, N., Chevallier, F., Chini, L. P., Evans, W., Florentie, L., Forster, P. M., Gasser, T., Gehlen, M., Gilfillan, D., Gkritzalis, T., Gregor, L., Gruber, N., Harris, I., Hartung, K., Haverd, V., Houghton, R. A., Ilyina, T., Jain, A. K., Joetzjer, E., Kadono, K., Kato, E., Kitidis, V., Korsbakken, J. I., Landschützer, P., Lefèvre, N., Lenton, A., Lienert, S., Liu, Z., Lombardozzi, D., Marland, G., Metzl, N., Munro, D. R., Nabel, J. E. M. S., Nakaoka, S.-I., Niwa, Y., O'Brien, K., Ono, T., Palmer, P. I., Pierrot, D., Poulter, B., Resplandy, L., Robertson, E., Rödenbeck, C., Schwinger, J., Séférian, R., Skjelvan, I., Smith, A. J. P., Sutton, A. J., Tanhua, T., Tans, P. P., Tian, H., Tilbrook, B., van der Werf, G., Vuichard, N., Walker, A. P., Wanninkhof, R., Watson, A. J., Willis, D., Wiltshire, A. J., Yuan, W., Yue, X., and Zaehle, S.: Global Carbon Budget 2020, Earth Syst. Sci. Data, 12, 3269–3340, https://doi.org/10.5194/essd-12-3269-2020, 2020.

Garbe, C. S., Rutgersson, A., Boutin, J., Leeuw, G. d., Delille, B., Fairall, C. W., Gruber, N., Hare, J., Ho, D. T., Johnson, M. T., Nightingale, P. D., Pettersson, H., Piskozub, J., Sahleé, E., Tsai, W.-t., Ward, B., Woolf, D. K., and Zappa, C. J.: Transfer across the air-sea interface, in: Ocean-Atmosphere Interactions of Gases and Particles, edited by: Liss, P. S. and Johnson, M. T., Springer, Berlin, Heidelberg, 55–112, 2014.

GLOBALVIEW-CO2: Cooperative Atmospheric Data Integration Project – Carbon Dioxide, 2008 version, NOAA ESRL, Boulder, Colorado, http://www.esrl.noaa.gov/gmd/ccgg/globalview/co2/, 2008.

https://doi.org/10.5194/essd-2021-16
Preprint. Discussion started: 29 March 2021

Gloege, L., McKinley, G.A., Landschutzer, P., Fay, A.R., Frolicher, T., Fyfe, J., Ilyina, T., Jones, S., Lovenduski, N.S., Rödenbeck, C., Rogers, K., Schlunegger, S., Takano, Y.: Quantifying errors in observationally-based estimates of ocean carbon sink variability, Global Biogeochemical Cycles, *in revision*, 2021.

Good, S. A., Martin, M. J., and Rayner, N. A.: EN4: Quality controlled ocean temperature and salinity profiles and monthly objective analyses with uncertainty estimates, *J. Geophys. Res. Oceans*, 118, 6704– 6716, doi:10.1002/2013JC009067, 2013.

Good S, Fiedler E, Mao C, Martin MJ, Maycock A, Reid R, Roberts-Jones J, Searle T, Waters J, While J, Worsfold M.: The Current Configuration of the OSTIA System for Operational Production of Foundation Sea Surface Temperature and Ice Concentration Analyses. *Remote Sensing*. 12(4):720, https://doi.org/10.3390/rs12040720, 2020.

Gregor, L., Lebehot, A. D., Kok, S., and Scheel Monteiro, P. M.: A comparative assessment of the uncertainties of global surface ocean CO2 estimates using a machine-learning ensemble (CSIR-ML6 version 2019a) – have we hit the wall?, Geosci. Model Dev., 12, 5113–5136, https://doi.org/10.5194/gmd-12-5113-2019, 2019.

Gregor, L., Fay, A. R.,: SeaFlux data set: Air-sea CO_2 fluxes for surface pCO_2 data products using a standardised approach. Zenodo, doi.org/10.5281/zenodo.4133802, 2021.

Gruber, N., Clement, D., Carter, B. R., Feely, R. A., van Heuven, S., Hoppema, M., Ishii, M., Key, R. M., Kozyr, A., Lauvset, S. K., Lo Monaco, C., Mathis, J. T., Murata, A., Olsen, A., Perez, F. F., Sabine, C. L., Tanhua, T., andWanninkhof, R.: The oceanic sink for anthropogenic CO2 from 1994 to 2007, Science, 363, 1193–1199, https://doi.org/10.1126/science.aau5153, 2019.

Hauck, J., Zeising, M., Le Quéré, C., Gruber, N., Bakker, D. C. E.,Bopp, L., Chau, T. T. T., Gürses, Ö., Ilyina, T., Landschützer, P., Lenton, A., Resplandy, L., Rödenbeck, C., Schwinger, J., and Séférian, R.: Consistency and Challenges in the Ocean Carbon Sink Estimate for the Global Carbon Budget, Front. Mar. Sci., 7, 1–33, https://doi.org/10.3389/fmars.2020.571720, 2020.

Hersbach, H., Bell, B., Berrisford, P., Hirahara, S., Horányi, A., Muñoz-Sabater, J., Nicolas, J., Peubey, C., Radu, R., Schepers, D., Simmons, A., Soci, C., Abdalla, S., Abellan, X., Balsamo, G., Bechtold, P., Biavati, G., Bidlot, J., Bonavita, M., De Chiara, G., Dahlgren, P., Dee, D., Diamantakis, M., Dragani, R., Flemming, J., Forbes, R., Fuentes, M., Geer, A., Haimberger, L., Healy, S., Hogan, R.J., Hólm, E., Janisková, M., Keeley, S., Laloyaux, P., Lopez, P., Lupu, C., Radnoti, G., de Rosnay, P., Rozum, I., Vamborg, F., Villaume, S., Thépaut, J.: The ERA5 global reanalysis. Q. J. R.Meteorol. Soc. 146, 1999–2049, doi: 10.1002/qj.3803, 2020.

Holding, T., Ashton, I. G., Shutler, J. D., Land, P. E., Nightingale, P. D., Rees, A. P., Brown, I., Piolle, J.-F., Kock, A., Bange, H. W., Woolf, D. K., Goddijn-Murphy, L., Pereira, R., Paul, F., Girard-Ardhuin, F., Chapron, B., Rehder, G., Ardhuin, F., and Donlon, C. J.: The FluxEngine air–sea gas flux toolbox: simplified interface and extensions for in situ analyses and multiple sparingly soluble gases, Ocean Sci., 15, 1707–1728, https://doi.org/10.5194/os-15-1707-2019, 2019.

Iida, Y., Takatani, Y., Kojima, A. and Ishii, M.: Global trends of ocean CO 2 sink and ocean acidification: an observation-based reconstruction of surface ocean inorganic carbon variables. *Journal of Oceanography*, pp.1-36, https://doi.org/10.1007/s10872-020-00571-5, 2020.

Jacobson, A. R., Mikaloff Fletcher, S. E., Gruber, N., Sarmiento, J. L., and Gloor, M.: A joint atmosphere-ocean inversion for surface fluxes of carbon dioxide: 1. Methods and global-scale fluxes, Global Biogeochem. Cycles, 21, GB1019, https://doi.org/10.1029/2005GB002556, 2007.

Kalnay, E., Kanamitsu, M., Kistler, R., Collins, W., Deaven, D., Gandin, L., Iredell, M., Saha, S., White, G.,Woollen, J., Zhu, Y.,
Chelliah, M., Ebisuzaki, W., Higgins, W., Janowiak, J., Mo, K. C., Ropelewski, C., Wang, J., Leetmaa, A., Reynolds, R., Jenne,
R., and Joseph, D.: The NCEP/NCAR 40-year reanalysis project, B. Am. Meteorol. Soc., 77, 437–470, 1996.

Kanamitsu, M., Kumar, A., Juang, H.M.H., Schemm, J.K., Wang, W., Yang, F., Hong, S.Y., Peng, P., Chen, W., Moorthi, S. and Ji, M.: NCEP dynamical seasonal forecast system 2000. *Bulletin of the American Meteorological Society*, *83*(7), pp.1019-1038, https://doi.org/10.1175/1520-0477(2002)083<1019:NDSFS>2.3.CO;2, 2002.

Key, R.M., Kozyr, A., Sabine, C.L., Lee, K., Wanninkhof, R., Bullister, J.L., Feely, R.A., Millero, F.J., Mordy, C. and Peng, T.H.: A global ocean carbon climatology: Results from Global Data Analysis Project (GLODAP). *Global biogeochemical cycles*, *18*(4), https://doi.org/10.1029/2004GB002247, 2004.

Kobayashi, S., Ota, Y., Harada, Y., Ebita, A., Moriya, M., Onoda, H., Onogi, K., Kamahori, H., Kobayashi, C., Endo, H., Miyaoka, K., and Takahashi, K.: The JRA-55 Reanalysis: General Specifications and Basic Characteristics, J. Meteorol. Soc. Jpn., 93, 5–48, https://doi.org/10.2151/jmsj.2015-001, 2015.

Krakauer, N. Y., Randerson, J. T., Primeau, F. W., Gruber, N. and Menemenlis, D.: Carbon isotope evidence for the latitudinal distribution and wind speed dependence of the airsea gas transfer velocity. Tellus B 58:390-417, https://doi.org/10.1111/j.1600-0889.2006.00223.x, 2006.

Lacroix, F., Ilyina, T., and Hartmann, J.: Oceanic CO2 outgassing and biological production hotspots induced by pre-industrial river loads of nutrients and carbon in a global modeling approach, Biogeosciences, 17, 55–88, https://doi.org/10.5194/bg-17-55-2020, 2020.

Landschützer, P., Gruber, N., Bakker, D. C. E., and Schuster, U.: Recent variability of the global ocean carbon sink, Global Biogeochemical Cycles, 28, 927–949, https://doi.org/10.1002/2014GB004853., 2014.

Landschützer, P., Gruber, N., Bakker, D. C. E.: An observation-based global monthly gridded sea surface pCO2 product from 1982 onward and its monthly climatology (NCEI Accession 0160558). Version 5.5. NOAA National Centers for Environmental Information. https://www.ncei.noaa.gov/access/ocean-carbon-data-system/oceans/SPCO2_1982_present_ETH_SOM_FFN.html. Dataset. https://doi.org/10.7289/V5Z899N6, 2020a.

Landschützer, P., Laruelle, G., Roobaert, A., and Regnier, P.: A combined global ocean pCO2 climatology combining open ocean and coastal areas (NCEI Accession 0209633), NOAA National Centers for Environmental Information, https://doi.org/https://doi.org/10.25921/qb25-f418, 2020b.

Laruelle, G. G., Landschützer, P., Gruber, N., Tison, J.-L., Delille, B., and Regnier, P.: Global high-resolution monthly pCO2 climatology for the coastal ocean derived from neural network interpolation, Biogeosciences, 14, 4545–4561, https://doi.org/10.5194/bg-14-4545-2017, 2017.

Laruelle, G. G., Cai, W. J., Hu, X., Gruber, N., Mackenzie, F. T., and Regnier, P.: Continental shelves as a variable but increasing global sink for atmospheric carbon dioxide, Nature Communications, 9(1), 454, https://doi.org/10.1038/s41467-017-02738-z, 2018.

McGillis, W. R., Edson, J. B., Hare, J. E., Fairall, C. W.: Direct covariance air-sea CO2 fluxes, J. Geophys. Res., 106(C8), 16,729–16,745, doi:10.1029/2000JC000506, 2001.

McKinley, G. A., Fay, A. R., Eddebbar, Y. A., Gloege, L., and Lovenduski, N. S.: External Forcing Explains Recent Decadal Variability of the Ocean Carbon Sink, AGU Adv., 1, 1–10, https://doi.org/10.1029/2019av000149, 2020.

Mikaloff Fletcher, S. E., Gruber, N., Jacobson, A. R., Doney, S. C., Dutkiewicz, S., Gerber, M., Follows, M., Joos, F., Lindsay, K., Menemenlis, D., Mouchet, A., Müller, S. A., and Sarmiento, J. L.: Inverse estimates of anthropogenic CO2 uptake, transport, and storage by the ocean, Global Biogeochemical Cycles, 20, GB2002, https://doi.org/10.1029/2005GB002530, 2006.

Müller, S. A., Joos, F., Plattner, G.-K., Edwards, N. R. and Stocker, T. F.: Modelled natural and excess radiocarbon - sensitivities to the gas exchange formulation and ocean transport strength. Global Biogeoch. Cycl. doi:10.1029/2007GB003065, 2008.

Naegler, T.: Reconciliation of excess 14C-constrained global CO2 piston velocity estimates. Tellus B 61, 372–384. doi: 10.1111/j.1600-0889.2008.00408.x, 2009.

Nightingale, P. D., Malin, G., Law, C. S., Watson, A. J., Liss, P. S., Liddicoat, M. I., Boutin, J., and Upstill-Goddard, R. C.: In situ evaluation of air-sea gas exchange parameterizations using novel conservative and volatile tracers, *Global Biogeochem. Cycles*, 14(1), 373– 387, doi:10.1029/1999GB900091, 2000.

Ramon, J., Lledó, L., Torralba, V., Soret, A. and Doblas-Reyes, F.J.: What global reanalysis best represents near-surface winds? *Quarterly Journal of the Royal Meteorological Society*, *145*(724), pp.3236-3251 https://doi.org/10.1002/qj.3616, 2019.

Resplandy, L., Keeling, R. F., Rödenbeck, C., Stephens, B. B., Khatiwala, S., Rodgers, K. B., Long, M. C., Bopp, L., and Tans, P. P.: Revision of global carbon fluxes based on a reassessment of oceanic and riverine carbon transport, Nat. Geosci., 11, 504–509, https://doi.org/10.1038/s41561-018-0151-3, 2018.

Rödenbeck, C., Keeling, R. F., Bakker, D. C. E., Metzl, N., Olsen, A., Sabine, C., and Heimann, M.: Global surface-ocean pCO2 and sea–air CO2 flux variability from an observation-driven ocean mixed-layer scheme, Ocean Sci., 9, 193–216, https://doi.org/10.5194/os-9-193-2013, 2013.

Roobaert, A., Laruelle, G. G., Landschützer, P., and Regnier, P.: Uncertainty in the global oceanic CO2 uptake induced by wind forcing: quantification and spatial analysis, Biogeosciences, 15, 1701–1720, https://doi.org/10.5194/bg-15-1701-2018, 2018.

Sarmiento JL, Gruber N: *Ocean biogeochemical dynamics*. Princeton University Press pp 526, 2006.

Shutler, J. D., Land, P. E., Piolle, J. F., Woolf, D. K., Goddijn-Murphy, L., Paul, F., Girard-Ardhuin, F., Chapron, B., and Donlon, C. J.: FluxEngine: A flexible processing system for calculating atmosphere-ocean carbon dioxide gas fluxes and climatologies, J. Atmos. Ocean. Tech., 33, 741–756, https://doi.org/10.1175/JTECH-D-14-00204.1, 2016.

Sweeney, C., Gloor, E., Jacobson, A. R., Key, R. M., McKinley, G.A., Sarmiento, J. L., Wanninkhof, R.: Constraining global air-sea gas exchange for CO2 with recent Bomb 14C measurements. Global Biogeoch. Cycl. 21, GB2015, doi:10.1029/2006GB002784, 2007.

Takahashi, T., Sutherland, S. C., Wanninkhof, R., Sweeney, C., Feely, R. A., Chipman, D. W., Hales, B., Friederich, G., Chavez, F., and Sabine, C.: Climatological mean and decadal change in surface ocean pCO2, and net sea–air CO2 flux over the global oceans, Deep-Sea Res. Pt. II., 56, 554–577, https://doi.org/10.1016/j.dsr2.2008.12.009, 2009.

Wanninkhof, R.: Relationship between wind speed and gas exchange over the ocean, J. Geophys. Res., 97, 7373, https://doi.org/10.1029/92JC00188, 1992.

Wanninkhof, R.: Relationship between wind speed and gas exchange over the ocean revisited, Limnol. Oceanogr.-Meth., 12, 351–362, https://doi.org/10.4319/lom.2014.12.351, 2014.

Watson, A. J., Schuster, U., Shutler, J. D., Holding, T., Ashton, I. G. C., Landschützer, P., Woolf, D. K., and Goddijn-Murphy, L.: Revised estimates of ocean-atmosphere CO2 flux are consistent with ocean carbon inventory, Nat. Commun., 11, 1–6, https://doi.org/10.1038/s41467-020-18203-3, 2020.

Weiss, R.: Carbon dioxide in water and seawater: the solubility of non–ideal gas. Mar. Chem. 2, 203–215, https://doi.org/10.1016/0304-4203(74)90015-2,1974.

Woolf, D. K., Land, P. E., Shutler, J. D., Goddijn-Murphy, L. M., and Donlon, C. J.: On the calculation of air-sea fluxes of CO_2 in the presence of temperature and salinity gradients, *J. Geophys. Res. Oceans*, 121, 1229– 1248, doi:10.1002/2015JC011427, 2016.

Zeng, J., Nojiri, Y., Landschützer, P., Telszewski, M. and Nakaoka, S.I.: A global surface ocean fco2 climatology based on a feed-forward neural network. *Journal of Atmospheric and Oceanic Technology*, *31*(8), pp.1838-1849, https://doi.org/10.1175/JTECH-D-13-00137.1, 2014.

https://doi.org/10.5194/essd-2021-16
Preprint. Discussion started: 29 March 2021

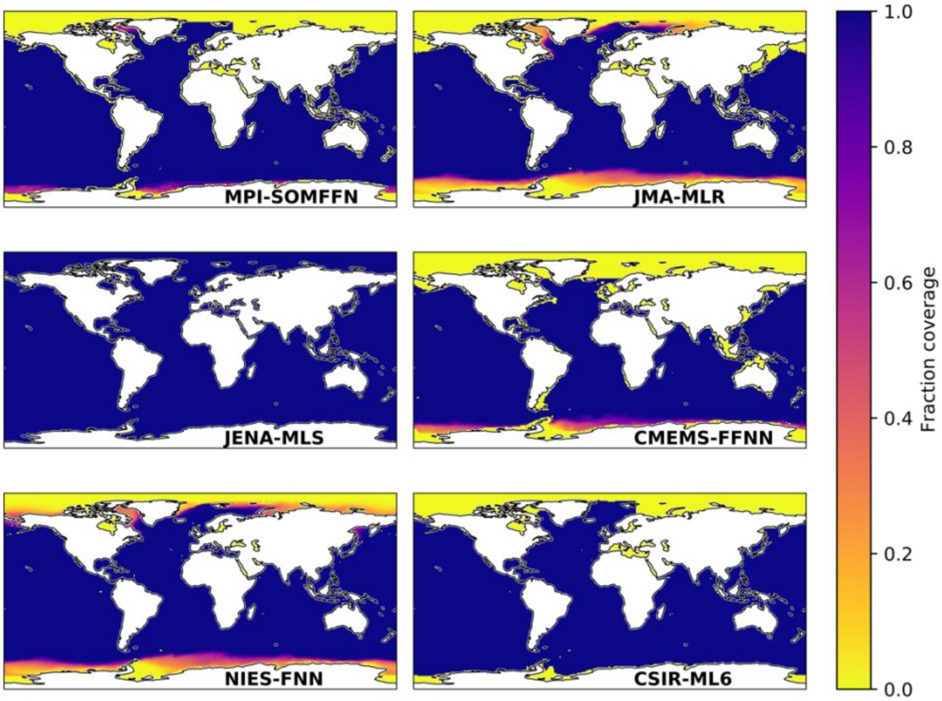

Figure 1: Maps showing the fraction of observations available as a function of time for the six pCO_2 data products used in this study. The products are resampled to a monthly resolution if required and are for years 1988 to 2018.

https://doi.org/10.5194/essd-2021-16
Preprint. Discussion started: 29 March 2021

Open Access Earth System Science Data Discussions

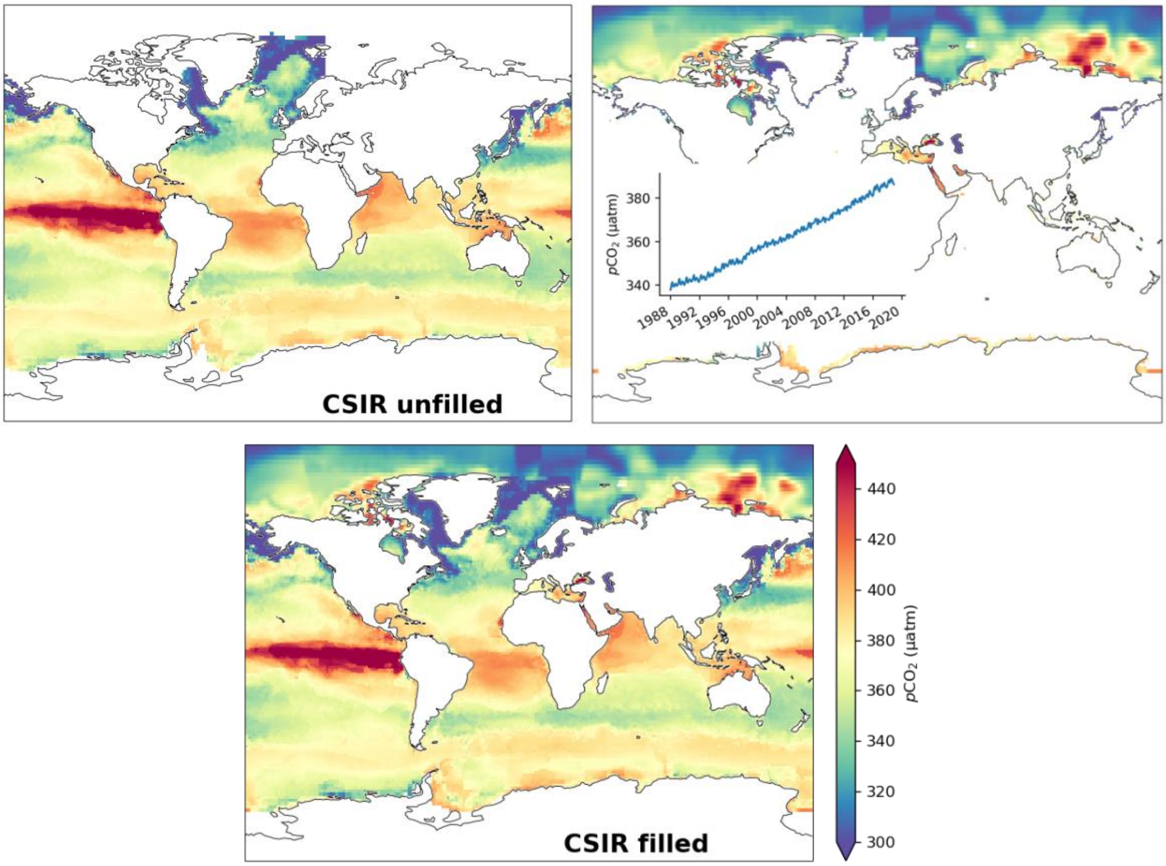

635 **Figure 2:** Maps demonstrating the filling procedure used in this study using a snapshot of pCO_2 from May 2013. (a) map of unfilled CSIR-ML6 pCO2. (b) the scaled pCO_2 climatology of Landschützer et al. (2020b) where the inlay shows the mean pCO_2 for the scaled climatology over time. (c) the CSIR-ML6 pCO_2 product (a) filled using the scaled climatology (b).

https://doi.org/10.5194/essd-2021-16
Preprint. Discussion started: 29 March 2021

Open Access Earth System Science Data Discussions

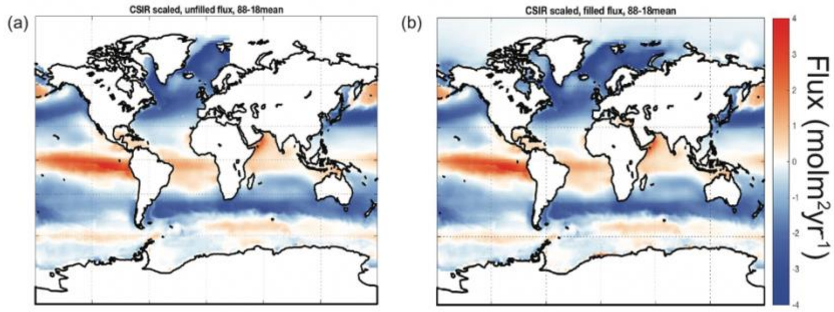

Figure 3: Mean flux (mol m^{-2} yr^{-1}), 1988-2018, for CSIR-ML6 product. (a) map of mean calculated flux using the original pCO_2 product and 3 scaled wind products; (b) map of mean calculated flux using the filled pCO_2 product and 3 scaled wind products. Similar maps for all other products are available in Figure A3.

https://doi.org/10.5194/essd-2021-16
Preprint. Discussion started: 29 March 2021

Open Access Earth System Science Data Discussions

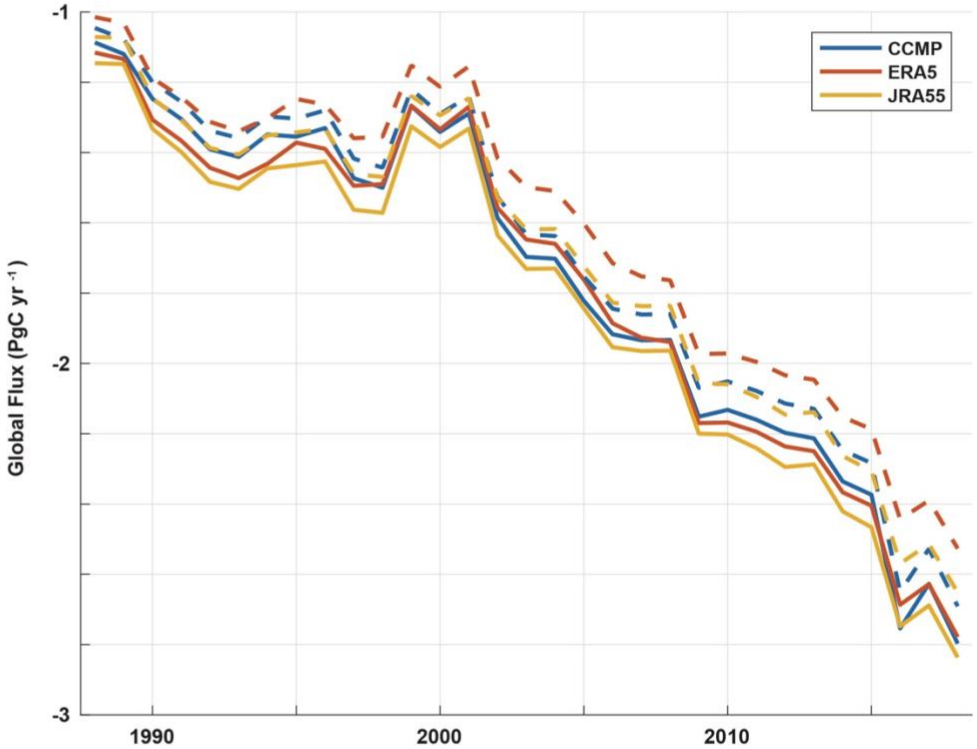

650 **Figure 4:** CSIR-ML6 product calculated air-sea CO_2 flux time series for various wind speed products; scaled (solid) and unscaled (dashed). Time series plots for all pCO_2 products and including 2 additional wind products (NCEP1 and NCEP2) are included in Figure A2.

https://doi.org/10.5194/essd-2021-16
Preprint. Discussion started: 29 March 2021

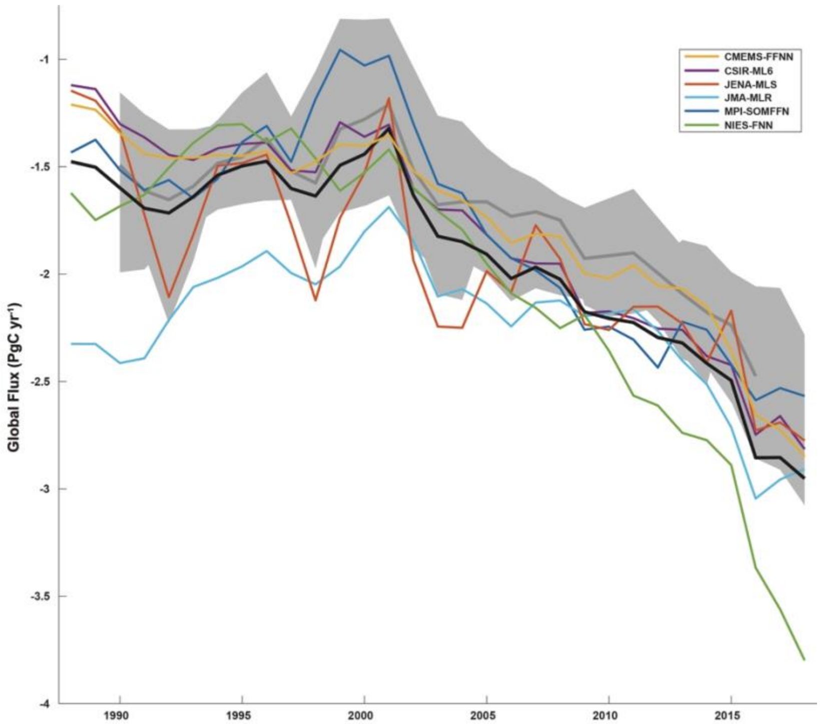

Figure 5: Global flux timeseries from six observation-based products. Colored lines show fluxes calculated from the standardized approach presented here (spatial filling with flux calculated from three wind products and the average flux is then plotted here); black line shows the mean of six products. Shaded region shows spread of original flux calculations from product creators with the mean represented as a gray line.

https://doi.org/10.5194/essd-2021-16
Preprint. Discussion started: 29 March 2021

Table 1: Global area coverage and mean pCO_2 for the six observation-based products. Unfilled area listed represents average area covered for 1988-2018 as this value changes monthly for many products (Figure A1). Change is defined as filled product – original product (i.e. a negative change implies the original product had a larger global/regional mean pCO_2 than the filled product).

Product	Area coverage (% global ocean)	Mean Global pCO_2 change (µatm)	Northern Hem pCO_2 change (µatm)	Southern Hem pCO_2 change (µatm)
CMEMS-FFNN *Denvil-Sommer et al. 2019* *Chau et al. 2020*	89%	-1.68	-4.35	0.30
CSIR-ML6 *Gregor et al. 2019*	93%	-0.93	-2.15	0.07
JENA-MLS *Rödenbeck et al. 2013*	100%	0.00	0.00	0.00
JMA-MLR *Iida et al. 2020*	85%	-0.69	-2.43	0.77
MPI-SOMFFN *Landschützer et al. 2014* *Landschützer et al. 2020a*	89%	-1.07	-2.62	0.16
NIES-FNN *Zeng et al. 2014*	92%	-0.36	-1.95	0.90

Table 2: CSIR-ML6 product flux values Flux values are from filled product. All values are computed over the period 1988-2018

Wind product	Scaled gas transfer coefficient (*a*)	Global flux mean (PgC yr^{-1})	Mean flux difference: scaled – unscaled winds
CCMP2	0.261	-1.77	-0.07
ERA5	0.276	-1.78	-0.16
JRA55	0.269	-1.83	-0.12

Table 3: Mean air-sea fluxes (PgC yr^{-1}), 1988-2018, using the mean of three wind products, calculated for the filled global area and the unfilled native "global" area for each pCO_2 product. The northern hemisphere (NH) and southern hemisphere (SH) fluxes (unfilled/filled) are included to highlight the imbalanced regional effect of the spatial filling process.

Product	Global Flux (unfilled/filled)	NH Flux (unfilled/filled)	SH Flux (unfilled/filled)
CMEMS-FFNN	-1.42/-1.79	-0.60/-0.92	-0.82/-0.84
CSIR-ML6	-1.65/-1.80	-0.78/-0.93	-0.87/-0.87
JENA-MLS	-1.94/-1.94	-1.00/-1.00	-0.94/-0.94
JMA-MLR	-1.98/-2.23	-0.92/-1.16	-1.06/-1.07
MPI-SOMFFN	-1.54/-1.77	-0.72/-0.94	-0.82/-0.84
NIES-FNN	-1.96/-2.04	-0.81/-0.90	-1.15/-1.14

https://doi.org/10.5194/essd-2021-16
Preprint. Discussion started: 29 March 2021

Open Access Earth System Science Data Discussions

Table 4: Mean fluxes (PgC yr^{-1}) for each observational pCO_2 product over the period 1988-2018. Mean flux calculated from filled coverage pCO_2 map and scaled gas exchange coefficient; global mean flux is for 3 wind products (CCMP2, ERA5, JRA55) and the
675 average. Time series of the mean flux values for each product (right most column) are plotted in Figure 5.

pCO_2 mapping Product	**CCMPv2**	**ERA5**	**JRA55**	**Mean**
CMEMS-FFNN	-1.73	-1.74	-1.79	-1.75
CSIR-ML6	-1.77	-1.78	-1.83	-1.79
JENA-MLS	-1.89	-1.90	-1.99	-1.93
JMA-MLR	-2.19	-2.21	-2.26	-2.22
MPI-SOMFFN	-1.75	-1.76	-1.81	-1.77
NIES-FNN	-2.00	-2.04	-2.07	-2.04
MEAN	-1.89	-1.90	-1.96	-1.92

https://doi.org/10.5194/essd-2021-16
Preprint. Discussion started: 29 March 2021

Appendix A

680 **Table A1:** Summary of parameters used to calculate flux

pCO_2 mapping Product	Wind speed product	Scaling of gas transfer value	Atmos surf pressure	Gas exchange Parameterization
This study	Calculated for three and final result is an average of the resulting fluxes: ERA5, JRA55, CCMP2	Scaled to 16.5 cm/hr	ERA5 Hersbach et al (2020)	Quadratic Wanninkhof (1992)
CMEMS-FFNN *Denvil-Sommer et al. 2019; Chau et al. 2020*	ERA5 Hersbach et al (2020)	Scaled to 16.0 cm/hr	CAMS inversion Chevallier (2013)	Quadratic Wanninkhof (1992)
CSIR-ML6 *Gregor et al. 2019*	ERA5 Hersbach et al (2020)	Scaled to 16.0 cm/hr	ERA5 Hersbach et al (2020)	Quadratic Wanninkhof (1992)
JENA-MLS *Rödenbeck et al. 2013*	NCEP1 Kalnay et al (1996)	Scaled to 16.5 cm/hr	NCEP1 Kalnay et al (1996)	Quadratic Wanninkhof (1992)
JMA-MLR *Iida et al. 2020*	JRA55 Kobayashi et al. (2015)	Scaled to 16.5 cm/hr	JRA55 Kobayashi et al. (2015)	Quadratic Wanninkhof (1992)
MPI-SOMFFN *Landschützer et al. 2020a*	ERA5 Hersbach et al (2020)	Scaled to 16.0 cm/hr	NCEP1 Kalnay et al. (1996)	Quadratic Wanninkhof (1992)
NIES-FNN *Zeng et al. 2015*	NCEP1 Kalnay et al. (1996)	Utilized *a* = 0.26 Takahashi et al. (2009)	NCEP1 Kalnay et al. (1996)	Quadratic Wanninkhof (1992)

https://doi.org/10.5194/essd-2021-16
Preprint. Discussion started: 29 March 2021

Table A2: Summary of wind products used in this study. Note that the date range starts for the first full year of data. We do not use NCEP1/2 in the main body of our study. Time units are in hours and space in degrees. Mean wind speed is given for the ice-free ocean.

Product name	**Resolution**		**Date range**	**Mean speed** ($m\ s^{-1}$)	**Scaling** (*a*)	**Reference**
	Time	**Space**				
Cross-Calibrated Multi-Platform v2	6	0.25	1988-present	7.7	0.261	Atlas et al. (2011)
ECMWF Reanalysis 5th Generation	1	0.25	1979-present	7.5	0.276	Hersbach et al. (2020)
Japanese 55-year Reanalysis	3	0.50	1958-present	7.6	0.269	Kobayashi et al. (2015)
NCEP-NCAR reanalysis 1	6	2.50	1948-present	7.2	0.293	Kalnay et al. (1996)
NCEP-NCAR reanalysis 2	6	2.50	1979-present	8.3	0.219	Kanamitsu et al. (2002)

https://doi.org/10.5194/essd-2021-16
Preprint. Discussion started: 29 March 2021

Open Access Earth System Science Data Discussions

Table A3: Mean fluxes, PgC yr^{-1}, 1988-2018 for each observational pCO_2 product. Mean flux calculated from unfilled (filled) coverage pCO_2 map and unscaled (scaled) gas exchange coefficient; calculated for 3 wind products (CCMP2, ERA5, JRA55) with the average shown here. Percent change is calculated as the difference between the unfilled/unscaled and filled/scaled as a fraction of the filled/scaled; does not indicate an error in the product's flux but is a representation of the impact the filling and scaling can have on the end flux estimate. The mean flux as reported in the original pCO_2 product is included for comparison (Figure 5).

pCO_2 mapping Product	Unfilled, unscaled	Filled, scaled	% change	Original product
CMEMS-FFNN	-1.33	-1.76	24%	-1.70
CSIR-ML6	-1.54	-1.80	14%	-1.51
JENA-MLS	-1.81	-1.94	6%	-1.91
JMA-MLR	-1.85	-2.22	17%	-1.59
MPI-SOMFFN	-1.45	-1.78	19%	-1.47
NIES-FNN	-1.84	-2.04	10%	-2.01

https://doi.org/10.5194/essd-2021-16
Preprint. Discussion started: 29 March 2021

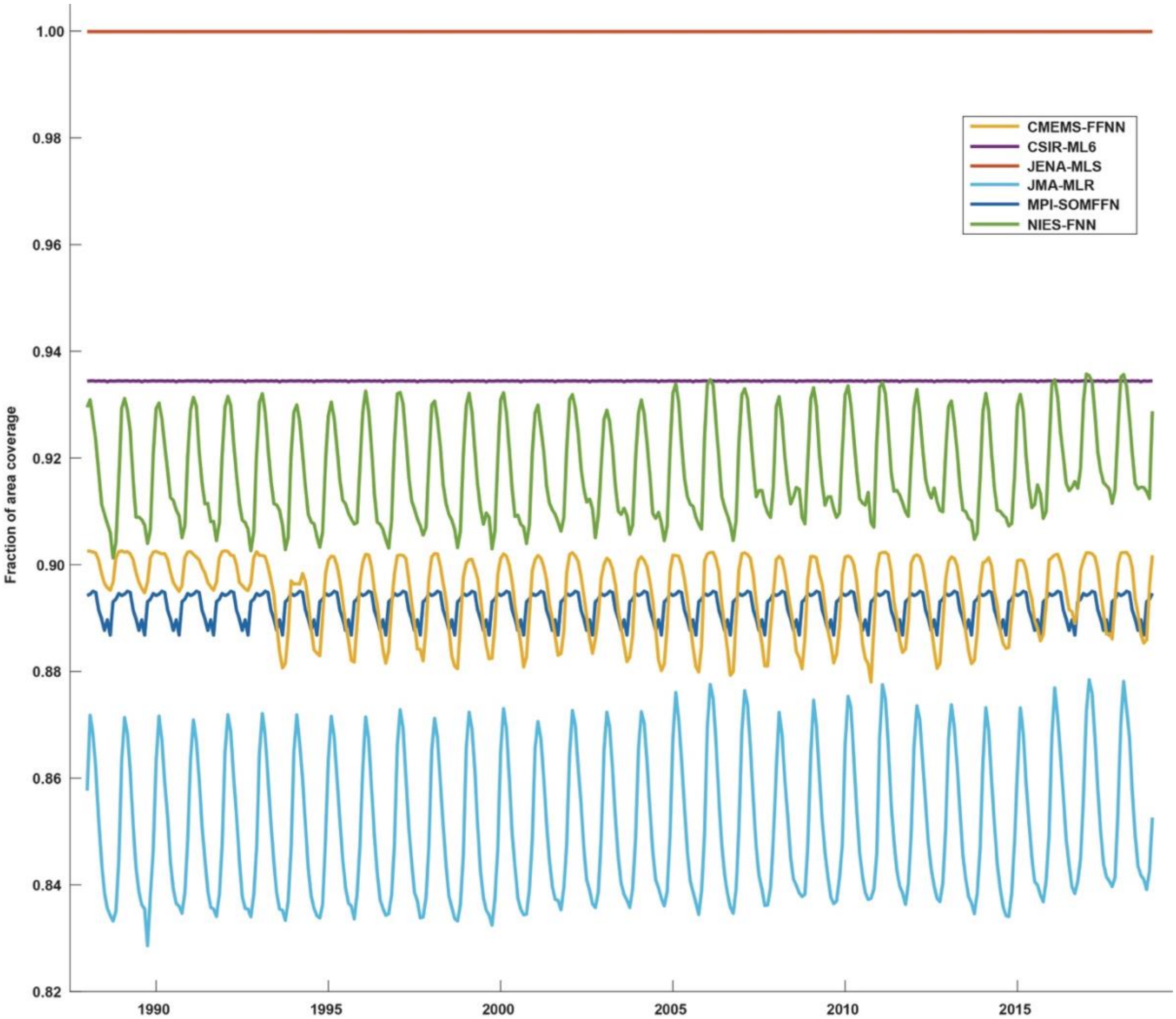

Figure A1: Time series showing the fraction of area covered by observations as a function of time (monthly) for the six pCO_2 data products used in this study.

https://doi.org/10.5194/essd-2021-16
Preprint. Discussion started: 29 March 2021

Open Access Earth System Science Data Discussions

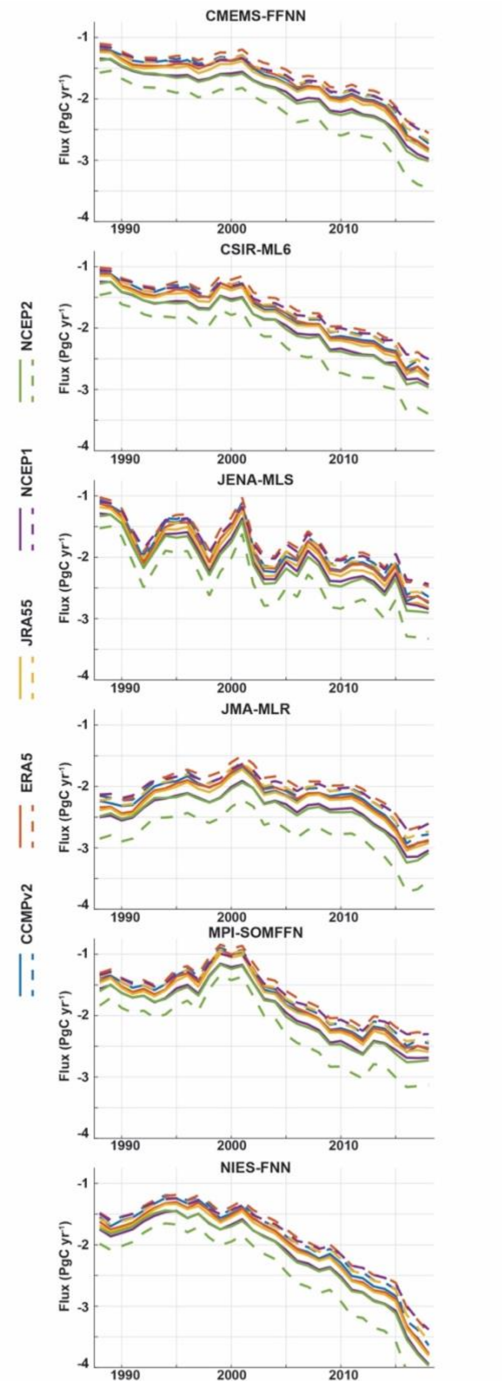

Figure A2: Air-sea CO_2 flux time series (PgC yr^{-1}) calculated using five wind speed products (CCMPv2, ERA5, JRA55, NCEP1,
705 NCEP2); scaled (solid) and unscaled (dashed).

https://doi.org/10.5194/essd-2021-16
Preprint. Discussion started: 29 March 2021

Open Access Earth System Science Data Discussions

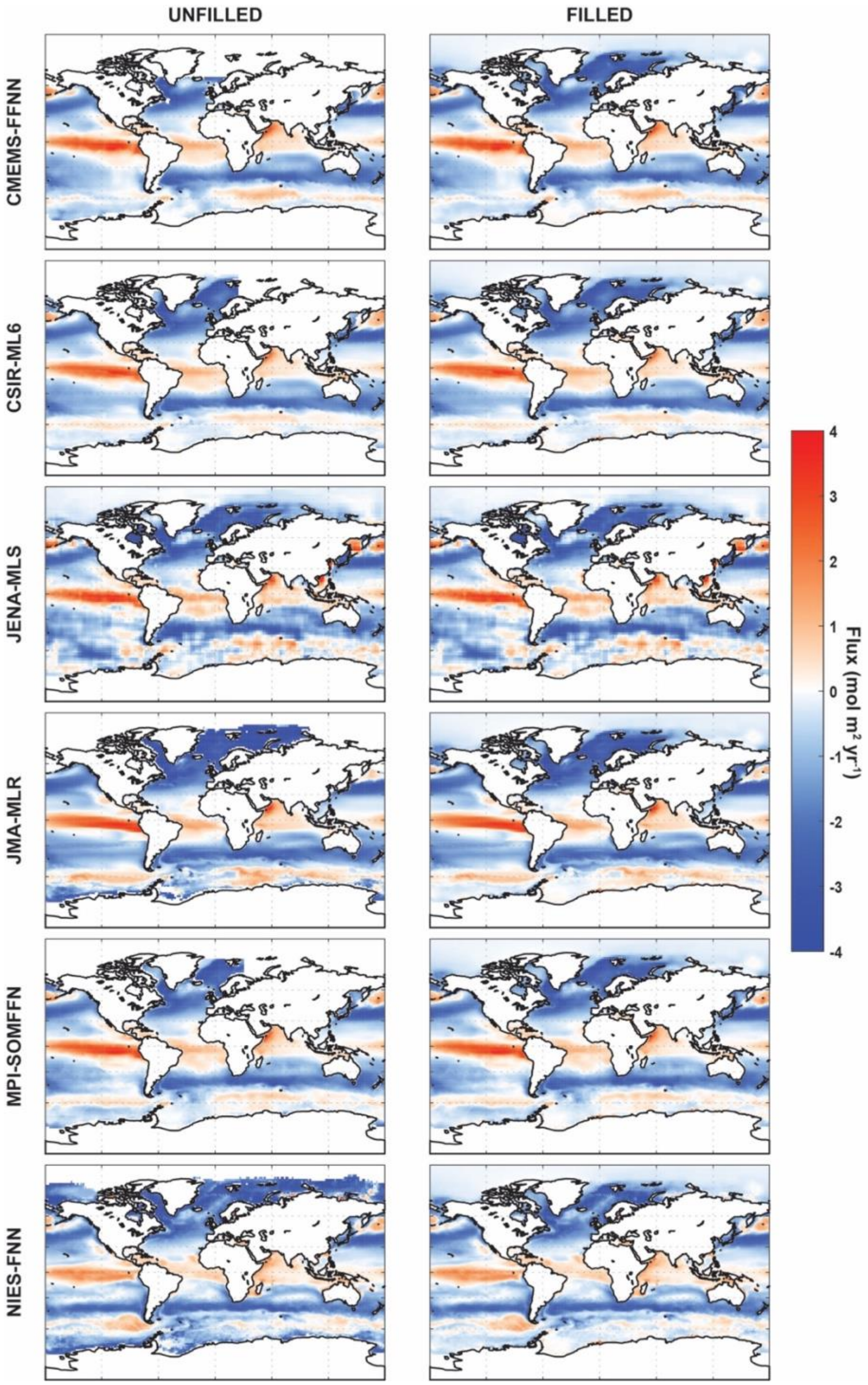

Figure A3: Mean flux (mol m^{-2} yr^{-1}), 1988-2018. Left hand column: map of mean calculated flux using the unfilled pCO_2 product and 3 scaled wind products. Right hand column: map of mean calculated flux using the filled pCO_2 product and 3 scaled wind products.